

Estimation of the Maximum Lateral Tire-Road Friction Coefficient Using the 6-DoF Sensor

Kyoung Seok Han¹, Eunjae Lee² and Seibum Choi^{3*}

^{1,2} School of Mechanical Aerospace & Systems Engineering, Division of Mechanical Engineering, KAIST, Daejeon, Korea

(Tel: +82-42-350-4160; E-mail: hks8804@kaist.ac.kr, asphaltguy@kaist.ac.kr)

³ School of Mechanical Aerospace & Systems Engineering, Division of Mechanical Engineering, KAIST, Daejeon, Korea

(Tel: +82-42-350-4160; E-mail: sbchoi@kaist.ac.kr)

Abstract: Estimated peak tire-road friction coefficient can be implemented on various vehicle active safety control systems. But, it is not easy to get the actual data from the road cause of cost, equipment installation, maintenance and technical issues. The demands for real-time estimation of peak friction coefficient have been increased due to the above mentioned technical shortcomings. This paper provides the lateral tire-road friction coefficient estimation method using a simplified Dugoff tire model under the pure side slip condition. The rearranged Dugoff model respect to lateral friction coefficient consists of lateral tire force, normal tire force, wheel side slip angle and cornering stiffness. Therefore, aforementioned parameters are also identified based on vehicle model or it is assumed to be constant values in the proposed algorithm. The performance of developed algorithm is verified by Carsim and Matlab/Simulink. The simulation results encourage possible development of the proposed method in this paper.

Keywords: tire-road friction coefficient, Dugoff tire model, pure side slip.

1. INTRODUCTION

The tire-road friction coefficient estimation is promising research area in automotive industry due to the increasing demands for vehicle safety system. There have been various estimation approaches from published studies. Those developed identification methods can be divided into two scheme according to vehicle motion. First scheme only considers vehicle longitudinal motion [1, 2] so their application area is restricted to longitudinal safety control system like Antilock Braking System (ABS). The remainder includes lateral dynamics in their estimation strategies [3, 4] but it contains intentional driver's brake or steering input for strategic purposes. In the real world, however, such a periodic driver inputs cannot be observed easily. Instead, sudden change of steering input is often occurred for various reasons. This paper mainly deals with those driving situations: ramp steering, step steering (no braking). The longitudinal tire force for individual wheels can be assumed to be negligible in the above mentioned driving conditions. Because longitudinal tire force and tire slip are inter-related but there is no slip when vehicle drives on the constant speed. By this way, we can concentrate on lateral tire-road friction coefficient assuming a tiny longitudinal friction coefficient. There has been similar estimation approach previously in [5]. Doumiati et al also neglected longitudinal force in their tire model but ultimate goal of this paper is estimation of lateral tire force, not road friction coefficient. Therefore, this paper assumed that friction coefficient on the proving ground is known value in their experimental verification. Jorge Villagra et al [6] took a similar estimation strategy using a Dugoff tire model [7]. However, algorithm

verification was done in the vehicle longitudinal motion under the pure slip condition. In this paper, simplified Dugoff tire model is used under the pure side slip condition. The maximum tire-road friction coefficient depends on vehicle lateral force and normal force in aforementioned situation.

Therefore accurate lateral/normal tire force estimation is also required. The 6-DoF inertial measurements are used to estimate lateral/normal tire force. The real-time lateral tire-road friction can be calculated after tire force estimation. Finally, the maximum tire-road friction coefficient, ultimate goal of this paper, is predicted based on real-time lateral friction coefficient. The estimated lateral friction coefficient can be used in vehicle lateral safety control system like Electronic Stability Control (ESC).

This paper is organized as follows. The simplified tire model is explained to develop the proposed identifier in Section 2. All sorts of parameters which are needed in this paper are estimated in Section 3. Simulation Results are shown in Section 4 using a Carsim and Matlab/Simulink. This paper is concluded in Section 5.

2. TIRE MODEL AND PARAMETER ADAPTATION CONCEPT

There are several tire model to reflect highly nonlinear phenomenon when vehicle generates tire force according to related parameters such as slip angle and slip ratio. A typical model from Pacejka, Magic Formula [8], gives a fully accurate results based on numerous experiments. However, this model has a lot of unknown parameter to be determined and its parameters are difficult to identify on real-time level. The Dugoff

tire-model is chosen in this paper because of its uncomplicated structure compared to Magic formula.

A complete expression for Dugoff model is as follows.

$$F_x = C_\sigma \cdot \frac{\sigma_x}{1 + \sigma_x} \cdot f(\lambda) \quad (1)$$

$$F_y = C_\alpha \cdot \tan(\alpha) \cdot f(\lambda) \quad (2)$$

where:

$$f(\lambda) = \begin{cases} (2 - \lambda)\lambda, & \lambda < 1 \\ 1, & \lambda > 1 \end{cases}$$

$$\lambda = \frac{\mu_{\max} F_z (1 + \sigma_x)}{2\sqrt{(C_\sigma \sigma_x)^2 + (C_\alpha |\tan(\alpha)|)^2}}$$

where C_σ is the longitudinal stiffness, C_α the cornering stiffness, σ_x the longitudinal slip ratio and α the wheel side slip angle.

The above tire model is developed based on integrated longitudinal and lateral tire model. However, in this paper, longitudinal tire force is assumed to be negligible. The simplified Dugoff tire model can be derived as follows under the pure side slip condition.

$$F_y = C_\alpha \cdot \tan(\alpha) \cdot f(\lambda) \quad (3)$$

where:

$$f(\lambda) = \begin{cases} (2 - \lambda)\lambda, & \lambda < 1 \\ 1, & \lambda > 1 \end{cases}$$

$$\lambda = \frac{\mu_{\max,y} F_z}{2C_\alpha |\tan(\alpha)|}$$

The lateral tire force has a linear property on low wheel side slip angle region and it is saturated at the behind of specific side slip as shown in Fig. 1. Nonlinear region on Fig. 1 has to be investigated because peak value is placed on these region, not linear region. Considering these aspects, (3) can be rearranged respective to lateral tire-road friction coefficient as follows.

$$F_y = C_\alpha \cdot \tan(\alpha) \cdot \left(2 - \frac{\mu_{\max,y} F_z}{2C_\alpha |\tan(\alpha)|}\right) \frac{\mu_{\max,y} F_z}{2C_\alpha |\tan(\alpha)|} \quad (4)$$

The maximum tire-road friction coefficient then can be written as below.

$$\mu_{\max,y} = \frac{2C_\alpha |\tan(\alpha)| \pm 2\sqrt{C_\alpha |\tan(\alpha)| (C_\alpha |\tan(\alpha)| - F_y)}}{F_z} \quad (5)$$

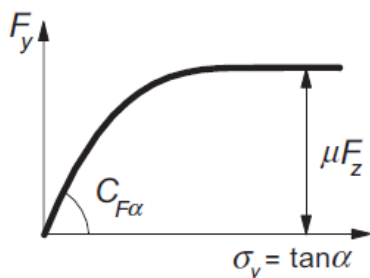


Fig. 1 Lateral tire force versus wheel side slip angle (5) has always positive solution because $C_\alpha |\tan(\alpha)| - F_y$ is always semi-positive.

In the aforementioned derived equation (5), lateral tire-road friction coefficient is dependent value with regard to lateral tire force, normal tire force, cornering stiffness and wheel side slip angle. Therefore, those parameter estimation has to be preceded.

3. PARAMETER ESTIMATION

3.1 Normal tire force estimation

The proposed individual normal tire force estimation method includes additional dynamic suspension effect and it incorporates all the vehicle's motion about 6-DoF. The estimated normal forces are made of static weight, longitudinal load transfer, lateral load transfer and suspension dynamic effect. The whole mass of vehicle is divided into four part as shown in Fig. 2 and all the component in (6) except static weight have different sign according to their mass position.

$$\hat{F}_{z,ij} = \underbrace{(m_{s,ij} + m_{u,ij})}_{\text{static weight}} g \pm \underbrace{\frac{(m_s + m_u) \ddot{x}_{cg} h}{2(l_f + l_r)}}_{\text{longitudinal load transfer}} \pm \underbrace{m_s \left(\ddot{z}_{cg} \pm l_f \ddot{\theta} \pm \frac{l_w}{2} \ddot{\phi} \right)}_{\text{suspension dynamic effect}} \pm \underbrace{m_u \ddot{z}_u \pm \frac{(m_s + m_u) \ddot{y}_{cg} h}{2l_w}}_{\text{lateral load transfer}} \quad (6)$$

where $F_{z,ij}$ is the vertical tire force at the individual wheel (i,j), $i \in \{F,R\}$, $j \in \{L,R\}$, m_s and m_u are sprung mass and un-sprung mass of quarter car model, h the height of the mass center, g the gravity acceleration constant, $\ddot{\theta}$ and $\ddot{\phi}$ are pitch and roll acceleration at the center of gravity, \ddot{z}_{cg} the normal acceleration, \ddot{y}_{cg} the lateral acceleration, \ddot{x}_{cg} the longitudinal acceleration at the center of gravity and l_f and l_r are distances from mass center to front and rear wheels, l_w the track width.

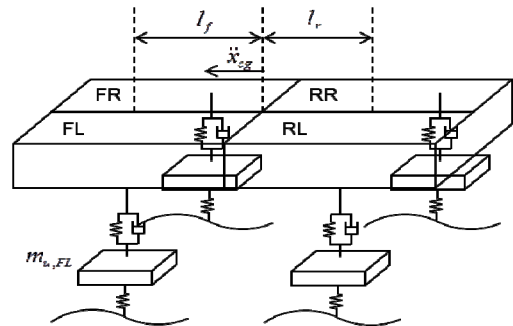


Fig. 2 Quarter car model.

All the normal tire force for quarter car model can be estimated with the above method ($\hat{F}_{FR}, \hat{F}_{FL}, \hat{F}_{RR}, \hat{F}_{RL}$). In this method, road disturbance such as bump and pothole can be considered using suspension dynamics.

3.2 Lateral tire force estimation

The lateral tire force for bicycle model can be written in terms of front and rear lateral force as (7), (8). Those relationship can be derived from Newton's second law of motion and procedure of derivation is well documented in [9].

$$\hat{F}_{yf} = \frac{ml_r a_y + I_z \dot{r}}{l_f + l_r} \quad (7)$$

$$\hat{F}_{yr} = \frac{ml_f a_y - I_z \dot{r}}{l_f + l_r} \quad (8)$$

Where $F_{y,f}$ and $F_{y,r}$ are the lateral tire forces of the front and rear wheels, a_y the lateral acceleration, \dot{r} the yaw acceleration and I_z the yaw inertia.

In this conventional way, the sum of each side hand lateral tire force can be calculated but the individual lateral tire force for each side hand also is needed to be determined.

The estimated lateral force can be distributed into both side according to their estimated normal tire force. However, it has a defect to apply directly in automotive industry due to their inaccuracy. In the future, distribution of those lumped lateral force is main residual task to implement the suggested algorithm in this paper.

3.3 Wheel side slip angle estimation

In [3], wheel side slip angle can be estimated from following equations in the front drive vehicle.

$$\begin{bmatrix} \alpha_{FL} \\ \alpha_{FR} \\ \alpha_{RL} \\ \alpha_{RR} \end{bmatrix} = \begin{bmatrix} \delta_{FL} \\ \delta_{FR} \\ \delta_{RL} \\ \delta_{RR} \end{bmatrix} - \tan^{-1} \begin{bmatrix} \frac{V_y + l_f r}{V_x} \\ \frac{V_y + l_f r}{V_x} \\ \frac{V_y - l_r r}{V_x} \\ \frac{V_y - l_r r}{V_x} \end{bmatrix} = \begin{bmatrix} \delta_f \\ \delta_f \\ 0 \\ 0 \end{bmatrix} - \tan^{-1} \begin{bmatrix} \beta + \frac{l_f}{V_x} r \\ \beta + \frac{l_f}{V_x} r \\ \beta - \frac{l_r}{V_x} r \\ \beta - \frac{l_r}{V_x} r \end{bmatrix} \quad (9)$$

where δ is the steering angle of wheel, β the vehicle side slip angle and r the yaw rate.

β cannot be directly measured in the production car so it is required to be identified as following method. Generally, bicycle dynamic model can be presented in terms of yaw rate and side slip angle [10] (Fig. 3).

$$\begin{aligned} \dot{x} &= Ax + Bu \\ y &= Cx \end{aligned} \quad (10)$$

where :

$$x = \begin{bmatrix} \beta \\ r \end{bmatrix}, u = \delta_f$$

$$A = \begin{bmatrix} a_{11} & a_{12} \\ a_{21} & a_{22} \end{bmatrix} = \begin{bmatrix} -\frac{2(C_f + C_r)}{mv_x} & \frac{2(C_r l_r - C_f l_f)}{mv_x^2} - 1 \\ \frac{2(C_r l_r - C_f l_f)}{I_z} & -\frac{2(C_f l_f^2 + C_r l_r^2)}{I_z v_x} \end{bmatrix}$$

$$B = \begin{bmatrix} b_1 \\ b_2 \end{bmatrix} = \begin{bmatrix} \frac{2C_f}{mv_x} \\ \frac{2C_f l_f}{I_z} \end{bmatrix}, C = [0 \quad 1]$$

where C_f, C_r are the cornering stiffness for rear/front wheel.

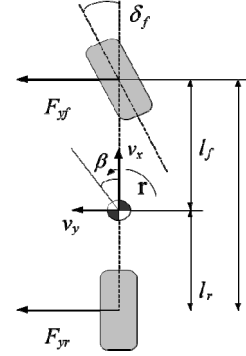


Fig. 3 Bicycle model for vehicle lateral dynamics.

In this paper, we assumed that inertia component and cornering stiffness are constant known value. The vehicle absolute velocity is almost same with wheel speed because of pure side slip condition. The yaw rate can be measured real-time in the production car.

Finally, the Luenberger observer can be constructed as follows.

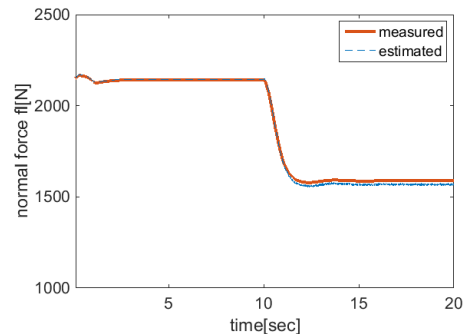
$$\dot{\hat{x}} = A\hat{x} + Bu + L(y - C\hat{x}) \quad (11)$$

In fact, estimation of vehicle side slip is also major issue in vehicle research area. All the relevant values, however, in (11) except for β are assumed to be known or measurable, and then the structure of dynamic equation has a suitable format to apply Luenberger observer.

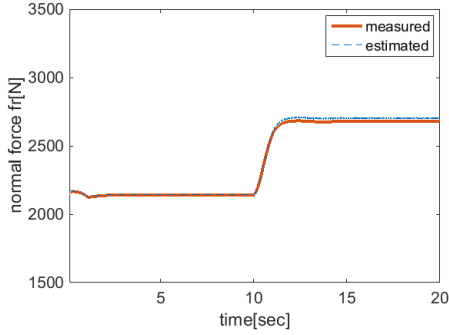
4. SIMULATION RESULTS

The performance of the proposed algorithm was verified by simulation using Carsim and MATLAB/Simulink. The target vehicle is an A-class model which is stored in Carsim and vehicle turns at 10sec with mild wheel steering angle input (ramp input : 0 to 30 degree during 5 seconds).

Fig. 4 shows that normal force estimation results for front wheel. The estimated values well track the measured values from Carsim. The significant lateral load transfer occurs at the 10 sec.

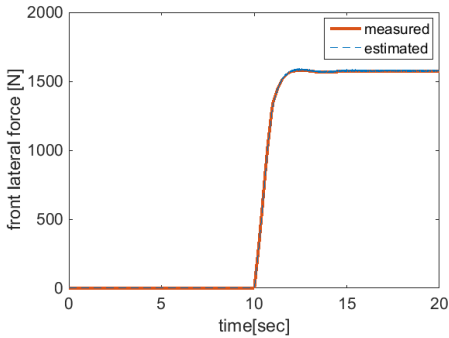


(a) Normal force for front left

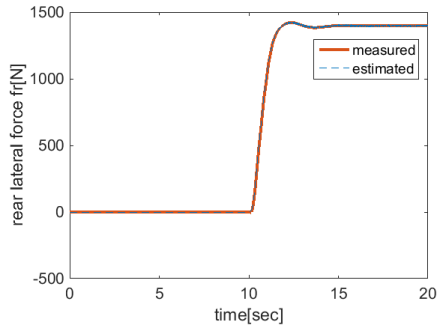


(b) Normal force for front right
Fig. 4 Normal force estimation results.

The estimation results from (7), (8) can be identified in Fig. 5. The sum of each side hand lateral forces is well estimated from bicycle model. However, distributed lateral tire forces according to their estimated normal force have minor error as shown in Fig. 6. As mentioned before, those estimation strategy should modified in the future for better performance regarding to each side hand lateral tire force.



(a) Front lateral force estimation (bicycle model)

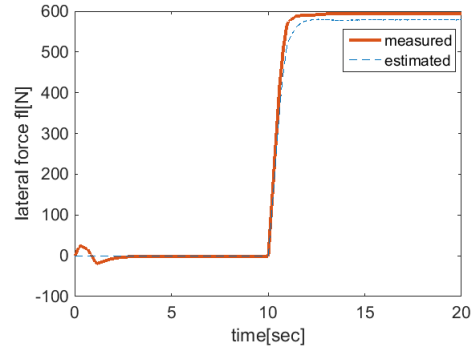


(b) Rear lateral force estimation (bicycle model)

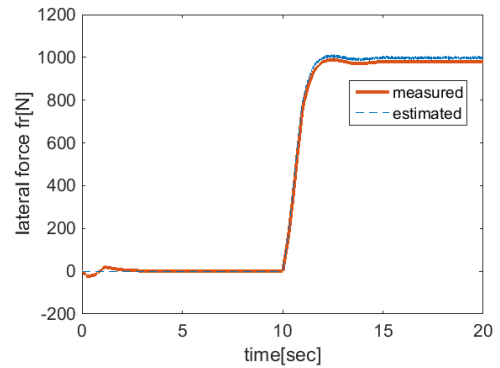
Fig. 5 Lateral tire force estimation using bicycle model.

If severe wheel steering input is exerted to vehicle, the estimation results of distributed lateral tire force might be more degraded. On the other hand, the lumped lateral force identification from bicycle model is almost same value with actual forces in any situation. In this simulation study, we assumed that mild steering input is exerted on vehicle so the estimated results can be used to be applied to Dugoff model. As mentioned before,

however, further study should be conducted to improve possibility of implementation.



(a) Front left lateral tire force (full model)



(b) Front right lateral tire force (full model)

Fig. 6 Distributed lateral tire force for each side hand.

The maximum tire-road friction estimation result from (5) is plotted in Fig. 7. After obtaining tire force information, lateral friction coefficient is identified under the pure side slip condition. The vehicle side slip angle starts to increase when the steering input is exerted around 10sec. The maximum friction coefficient can be determined from Dugoff tire model and it can be identified more quickly than measured value from ratio of normal force and lateral ($\mu_y = F_y / F_z$) force.

The measured value cannot reach the maximum lateral tire-road friction coefficient due to insufficient wheel side slip angle. The peak friction coefficient can be observed at the specific wheel side slip angle as shown in Fig. 1. The steering input is not fully to reach peak value in this simulation environment. On the other hand, estimated value can identify real value because of tire-model structure. The quick tire-road friction identification than conventional method (measured value) is demonstrated in this simulation study, whose ultimate goal of this paper.

In fact, tire-road friction coefficient estimation result has a meaningful value before tire-force saturation. The real-time friction coefficient can be identified easily through conventional method but the peak value identification in the low wheel side slip angle region is more important in the view of vehicle lateral control. Those task was realized in this paper using Dugoff tire model.

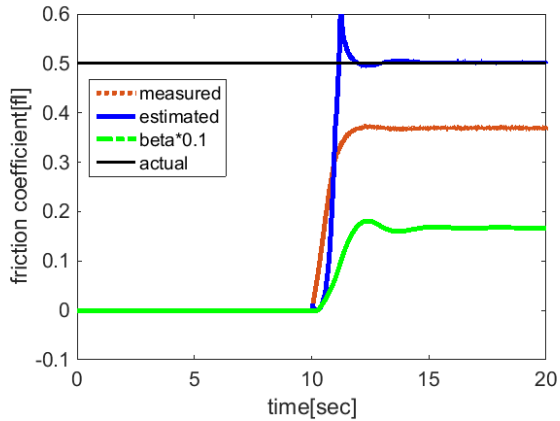


Fig. 7 Tire-road friction coefficient estimation on medium μ ($\mu_{\max}=0.5$)

In order to verify the robustness of the proposed algorithm, simulation studies are continued on the low μ road surface (0.3) as shown in Fig. 8. All the simulation environment is identical to Fig. 7 except for friction coefficient. The result shows similar tendency with the result on the medium μ (0.5). The estimated value can reach the real maximum friction coefficient, but measured value cannot identify the μ .

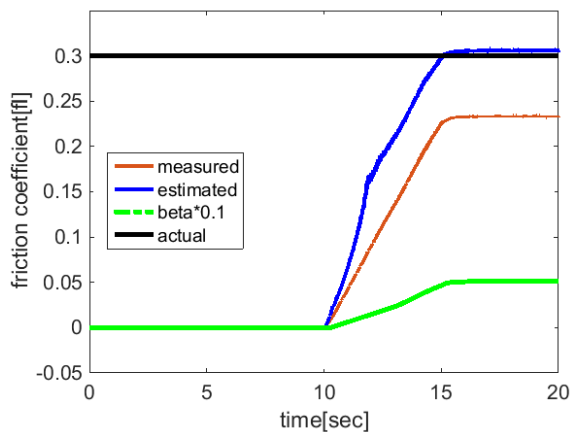


Fig. 8 Tire-road friction coefficient estimation on medium μ ($\mu_{\max}=0.3$)

5. CONCLUSION

This paper presents maximum tire-road friction coefficient estimation method using 6DoF sensor measurements. The main advantage of the proposed algorithm is that maximum friction coefficient can be identified quickly than conventional method. The lateral tire force distribution study should be done in the future for algorithm robustness. In the simulation studies, the homogenous road surface is only considered due to an imperfect knowledge of split lateral tire force. The distribution of the lumped lateral tire force wasn't attained in this paper. The algorithm verification was not conducted in the split μ . The estimated value, however, match well in the homogenous road surface.

ACKNOWLEDGEMENT

This research was supported by the MSIP(Ministry of Science, ICT and Future Planning), Korea, under the C-ITRC (Convergence Information Technology Research Center) (IITP-2015-H8601-15-1005) supervised by the IITP(Institute for Information & communications Technology Promotion) and This work was supported by the National Research Foundation of Korea(NRF) grant funded by the Korea government(2010-0028680)

REFERENCES

- [1] R. Rajamani, "Friction estimation on highway vehicles using longitudinal measurements," 2004.
- [2] K. Yi, K. Hedrick, and S.-C. Lee, "Estimation of tire-road friction using observer based identifiers," *Vehicle System Dynamics*, vol. 31, pp. 233-261, 1999.
- [3] M. Choi, J. J. Oh, and S. B. Choi, "Linearized Recursive Least Squares Methods for Real-Time Identification of Tire-Road Friction Coefficient," *Vehicular Technology, IEEE Transactions on*, vol. 62, pp. 2906-2918, 2013.
- [4] J.-O. Hahn, R. Rajamani, and L. Alexander, "GPS-based real-time identification of tire-road friction coefficient," *Control Systems Technology, IEEE Transactions on*, vol. 10, pp. 331-343, 2002.
- [5] M. Doumiati, A. C. Victorino, A. Charara, and D. Lechner, "Onboard real-time estimation of vehicle lateral tire-road forces and sideslip angle," *Mechatronics, IEEE/ASME Transactions on*, vol. 16, pp. 601-614, 2011.
- [6] J. Villagra, B. d'Andréa-Novel, M. Fliess, and H. Mounier, "A diagnosis-based approach for tire-road forces and maximum friction estimation," *Control engineering practice*, vol. 19, pp. 174-184, 2011.
- [7] H. Dugoff, P. Fancher, and L. Segel, "An analysis of tire traction properties and their influence on vehicle dynamic performance," SAE Technical Paper1970.
- [8] H. Pacejka, *Tire and vehicle dynamics*: Elsevier, 2005.
- [9] R. Rajamani, *Vehicle dynamics and control*: Springer Science & Business Media, 2011.
- [10] J. Oh, S. Choi, and D. Kim, "Disturbance observer design based on linearized vehicle model for unequal tractive/braking force identification," in *Control, Automation and Systems (ICCAS), 2012 12th International Conference on*, 2012, pp. 567-572.